

Development of the methodology for the Detection and Quantification of Zinc Oxide Nanoparticles and dissolved Zinc by Single-Particle Inductively Coupled Plasma Mass Spectrometry

Lisia Maria Gobbo dos Santos

lisia.gobbo@fiocruz.br

Instituto Nacional de Controle de Qualidade em Saúde

Cristiane Barata-Silva

Instituto Nacional de Controle de Qualidade em Saúde

Santos Alves Vicentini-Neto

Instituto Nacional de Controle de Qualidade em Saúde

Fabio Silvestre Bazilio

Instituto Nacional de Controle de Qualidade em Saúde

André Luiz O. Silva

Agência Nacional de Vigilância Sanitária

Silvana Couto Jacob

Instituto Nacional de Controle de Qualidade em Saúde

Josino Costa Moreira

Oswaldo Cruz Foundation

Research Article

Keywords: SP-ICP-MS, nanoparticles, validation, Zinc

Posted Date: April 22nd, 2024

DOI: <https://doi.org/10.21203/rs.3.rs-4271920/v1>

License:  This work is licensed under a Creative Commons Attribution 4.0 International License.

[Read Full License](#)

Additional Declarations: No competing interests reported.

Version of Record: A version of this preprint was published at Journal of Nanoparticle Research on October 7th, 2024. See the published version at <https://doi.org/10.1007/s11051-024-06151-8>.

Abstract

The increasing production of zinc oxide nanoparticles and their use in products of sanitary interest make the analysis and characterization extremely important from the point of view of public health and environmental risk. This work aimed to validate the methodology using SP-ICP-MS to measure and quantify nanoparticles of ZnONPs and dissolved zinc -Zn(i). This study pointed out that the method was suitable for the purpose, presenting satisfactory results for the recovery and precision test for Zn (i) and size of NPs. The limits of detection size, dissolved zinc concentration, and particle concentration were 67 nm, $0.4 \mu\text{g L}^{-1}$, $1.08 \times 10^5 \text{ particles mL}^{-1}$, respectively. Thus, the results obtained demonstrate that the technique can be used to determine the size and concentration of Zn(i) in different products.

Introduction

Studies in nanotechnology began in 1981 and are still growing today due to their applications in different areas.(1, 2). Pioneer products in the development of the use of nanoparticles (NP) in cosmetics were sunscreens containing zinc oxide (ZnO) and titanium dioxide (TiO₂) in the form of engineered nanoparticles (ENPs), as these form a physical barrier against UVA and UVB radiation in addition to having the ability to become invisible after application, which increase the aesthetically appealing to consumers.(3–5). Despite their useful properties, the dangers of nanoparticles in the biological system are still poorly understood, and their potential harmful effects on living organisms must be studied(6).

One of the most promising techniques for analyzing metallic nanoparticles is inductively coupled plasma mass spectrometry (ICP-MS). This technique was able to reinvent itself as a particle counting technique, just by using very high data acquisition frequencies to measure nanoparticle suspensions sufficiently diluted (7–9). Under such conditions, ICP-MS is able to provide information on a particle-by-particle basis, giving rise to the so-called single-particle ICP-MS (SP-ICP-MS) (10, 11). The 'single particle' module allows real-time data acquisition and provides analytical information for quantitative analyses as measurement of the number concentration, mass concentration of nanoparticles concentration, and mass concentration of dissolved ions, furthermore this technique provides information by characterization of nanoparticles and histogram showing the number of particle for each of number of define size classes (12–14).

The basic principle of the SP-ICP-MS technique consists of the individual detection of nanoparticles, introduced in diluted suspensions with a high frequency of detector measurements, statistically causing only one nanoparticle to enter the plasma at a time (12). The nanoparticles that reach the plasma form a mass of ions proportional to their size, and when they reach the detector, they generate a pulse with greater intensity than the continuous measurement of the dissolved metal. The size of each nanoparticle can then be calculated from the corresponding pulse intensity (15, 16).The SP-ICP-MS has been gaining recognition because of the increasing number of related publications, describing the principle of the technique, and mainly applications in samples from different sources (17).

An important point to consider in any analytical analysis is the reliability of measurements carried out in chemical laboratories. It is necessary to validate the analytical method to guarantee that the obtained results are valid. For this objective, the parameters to be followed, such as linearity and working range, precision, selectivity, detection limit and accuracy, are recommended by ISO/IEC 17025 (18, 19). These parameters are used for mass/number concentration validation, but also to particle size (20).

Experimental

Standards and Reagents

A standard $999 \pm 2 \mu\text{g L}^{-1}$ dissolved Zn stock solution in 5% HNO_3 (Sigma-Aldrich, Saint Louis, MO, USA) was used to prepare an intermediate $100 \mu\text{g L}^{-1}$ solution. The calibration curve was prepared in 15 mL Falcon flasks using successive dilutions in ultrapure water.

Monodisperse ZnONP suspensions were prepared from commercially available solutions. ZnONPs measuring $< 100 \text{ nm}$ particle size (DLS) $> 35 \text{ nm}$ avg. part size (APS), 50 wt. % in H_2O . (Sigma Aldrich, Missouri, EUA). After dilution and before each analysis, the suspensions were sonicated and vortexed for 1 min.

AuNP standard solution of nominal size of 50 nm, supplied by NanoComposix (San Diego, CA, USA), was used to validate the TE, it is not required to use de nanoparticle the same element that will be analysis (21).

For the quality assurance of the result, Water 1643F acquired from the National Institute of Standards and technology (Nist) was used for evaluating the accuracy, precision, and recovery study.

Instrumentation

The experiments were performed on a NexION 300D ICP-MS (Perkin Elmer, USA), equipped with a concentric nebulizer type Meinhard, glass cyclonic nebulizer chamber, cone, skimmer, and nickel hyper-skimmer. ICP-MS instrumental and data acquisition parameters are listed in Table 1. Although ^{67}Zn has a lower natural abundance than the other Zn isotopes, it was chosen to avoid $^{50}\text{Ti}^{16}\text{O}$ interference that occurs with the ^{66}Zn isotope and is found in greater abundance (22, 23).

In the ICP-MS technique, only a fraction of the nebulized suspension effectively reaches the plasma (1–15%) when using conventional systems, and this, too, happens in the single particle mode (24). The precise determination of this fraction, defined as transport efficiency (TE), is critical for correctly determining both particle number concentration and size (25). The TE was calculated by the particle frequency (TEF) methods using an AuNP standard solution of nominal size of 50 nm, which was sonicated for 1 min and diluted 100-fold in deionized water (Milli-Q Advantage, Molsheim, France) to a final nominal concentration of $1 \times 10^5 \text{ particles mL}^{-1}$, supplied by NanoComposix (San Diego, CA, USA).

The interday repeatability of TE was calculated, and the mean was used for validation. The variations found can be strongly influenced by the daily optimization procedures of the ICP-MS instrument.

In developing the methodology, we applied two complementary approaches to ensure the precision and efficacy of the analytical process. The waste collection technique was employed to ensure accuracy in the volume of sample aspirated, a critical factor for the reliability of nanoparticle quantification results. Concurrently, the particle frequency approach was utilized to optimize the transport efficiency (TE), ensuring our SP-ICP-MS system could detect and quantify nanoparticles with the highest precision possible. Although these strategies serve different purposes, both are fundamental to the integrity of our results, demonstrating the rigor and robustness of our analytical methodology (24, 26).

The Zn total (t-Zn) concentration was determined by inductively coupled plasma optical emission spectrometry – ICP OES – model Optima 8300 (Perkin Elmer, USA) equipped with a GemCones™ nebulizer, cyclonic glass nebulizer chamber.

Table 1
Default single particle inductively coupled plasma mass spectrometry
instrumental and data acquisition parameters.

Instrumental parameters		
RF Power	1400 W	
Argon gas flow rate		
Plasma	18 L min ⁻¹	
Auxiliary	1.2 L min ⁻¹	
Nebulizer	1 L min ⁻¹	
Data acquisition parameters		
Measurement unit	Standard	Single particle detection
Point per spectral peak	1	1
Sweeps	20	1
<i>Dwell time</i>	50 ms	50 μs
Readings per replicate	1	2000.000
Integration time	1 s	100 s
Method Parameter	Zn	
Isotope (amu)	67	
Density (g/cm ³)	5.61	
Mass Fraction (%)	80.31	
Ionization Efficiency (%)	100	

Sample preparation

The lack of reference certified materials for NP in different matrixes, led us to use recovery tests to fulfill the validation requirements. A spiking control sample with NP standards and ion dissolved standards were used to evaluate the accuracy and precision. A sunscreen sample that declared on the label no ZnONP was used as negative control. 0.30 g of the sample was weighed (triplicate) and submitted to two hours ultrasonic treatment, followed by centrifugation at 5,000 rpm for 30 min, and filtration through 0.22 μm pore membranes. After filtration, each sample was sonicated and vortexed for 1 min. The same extraction process was applied to a blank solution containing only ultrapure water.

The t-Zn determination was made, weighing approximately 0.5 g of ZnONP suspensions in triplicate. The samples were transferred to Teflon tubes containing 2 mL of deionized water (Millipore, Brazil), 2 mL of

65% (w/v) nitric acid (Merck, Germany), and 2 mL of 30% hydrogen peroxide (v/v) (Merck). The sample digestion was made using microwaves in an enclosed high-pressure system, SpeedWave microwave (Berghof, Germany), and after chilling, the samples were transferred to 50 mL volumetric flasks (27).

Preparation of the analytical curve

Five analytical curves were prepared using a Zn standard dissolved in a concentration range from 1 to 20 $\mu\text{g L}^{-1}$. The samples were determined in SP-ICP-MS mode, and the analytical curve of dissolved Zn was crafted considering the relationship between the signal strength (counts) and mass per event ($\mu\text{g}/\text{event}$), converted by equipment software.

Selectivity

The selectivity of the technique was determined by matrix effect (standard addition). Two distinct groups containing Zn ions were prepared, a group of the matrix of interest (group 1) with known concentration of the analyte, and another group made up of water and the analyte (group 2) (25).

Limited of detection

ZnONP identification and quantification by SP-ICP-MS depends on two factors: (i) the size of the NP, which must be large enough to generate several ions detectable by the spectrometer, and (ii) the numerical NP concentration, which must be high enough to allow counting a minimum number of events (24). Therefore, three LODs are calculated: the LOD size (LOD_d) for the diameter of NPs, the concentration of the number of NPs LOD (LOD_p), and LOD for ion dissolved zinc (Zn(i)). The limits of detection were obtained by reading of ten solutions independent of the blank and calculated according to studies published by Laborda *et al.*, 2020, using parameters such as TE, dwell time, flow rate, time integration, sensibility of ion concentration (slope of concentration curve), count number of particle and mean of baseline signal (21, 25, 26, 28).

The limit of quantification (LOQ) for zin(i) was obtained experimentally, defined as the first point of the calibration curve (20).

Accuracy and precision

The method's accuracy was determined by the analysis of ZnONP standards by two different techniques: ICP OES and ICP-MS. t-Zn results were evaluated by application of Student's t-test. The results indicated there is no significant difference between the results ($p > 0.05$). The average ZnO concentration is equal to 44.8 g L^{-1} . The theoretical number of nanoparticles/mL (3.7×10^{13} particles mL^{-1}) was determined using the average ZnO concentration. It was possible to calculate the declared average size of the certified standard (75nm) (23).

To assess the method's accuracy and precision, a sample of Nist 1643F and sunscreen were prepared to contain ZnONPs and dissolved Zn. The Zn(i) concentration was chosen to have a concentration in the middle of the calibration curve, and the ZnONP concentration was close to the LOD. The solutions were

analyzed five times by SP-ICP-MS, and the average amount of particles, size, and Zn (i) concentration for each sample was compared with the theoretical results.

Statistical analyses

Descriptive statistics were obtained using Microsoft Excel, including arithmetic mean, median, standard deviation (SD), Student's t-test, and analysis of variance (ANOVA). The uncertainty was estimated by adopting the 'bottom-up' method, which starts with identifying and characterizing the individual sources of uncertainty and then combines them to obtain the total uncertainty. The main sources are represented in Fig. 1, where the repeatability of the methodology is associated with random effects and was verified by the standard deviation of the response and quantified from repeated experiments and verified by the standard deviation of the response; sample preparation is associated with calibration uncertainties obtained from the calibration certificates of the volumetric flask and analytical balance used; the uncertainty of the standards is associated with the uncertainty of the stock solution purchased and the calibration certificates of the volumetric flask and pipettes used, and the uncertainty of the calibration curve is associated with the uncertainty of the angular coefficient (30). Once the coverage factor k ($k = 2$) was set at a 95% confidence level and the final combined uncertainties were estimated, the final expanded uncertainty was calculated (18, 19).

Results and Discussion

The optimized parameters were dwell time (50 μs), integration time (100 s) and sample flow rate (0.20 mL min^{-1}). The waste collection method was used to indirectly determine the flow, by calculation of the ratio between the total volume captured and the difference between the uptake sample and the waste volume after 60s of aspiration. (20). This process was repeated ten times, and the variation among results was less than 5%, indicating the precision of the method (26).

The average TE result was $8.3 \pm 1.1\%$. To minimize the impact of NP losses to the container walls and the sample introduction system, the NP suspensions were daily prepared in a conditioned container (repeated dilution of the stock suspension into the same container) additionally, the losses in the sample introduction system were minimized by the use of short tubes and long sample discharge times (24).

Analytical curve

The dissolved Zn concentrations were correlated to the Zn mass with reference to each reading ('dwell time'), transport efficiency in % and sample flow in mL s^{-1} (29) to define the mass flow curve for NP quantification. The linearity was determined with the support of the by Bazilio's *et al.* document "Worksheet for Assessing Assumptions" (30). The results pointed out the curve regression is significant ($p > 0.05$ indicate's no linearity deviation). The coefficient of determination (R^2) was 0.9980, indicating that the analytical curve presents adequate linearity according to INMETRO specifications (19, 30).

Selectivity

Through the results obtained, the Snedecor F-test of homogeneity of variances and Student's *t*-test for comparison of means were applied. The *t*-test value was below of the the expected value (*t critic*) and it indicates that the matrix does not have a statistically significant effect on the results with a 95% confidence (*p-value* > 0,05%) (25, 31).

Limited of detection

The determined LOD for zinc (i) was $0.4 \mu\text{g L}^{-1}$. LOD was calculated, in the single particle mode, applying the ratio of three times the standard deviation of blank sample (ultrapure water) by the sensitivit (28, 31).

The limit of detection for size (LOD Sizes) represents the smallest size of particle capable of generating a signal tree times higher than noise (24). Factors such as the concentration dissolved element, the baseline signal and the type of de spectrometer influence the LOD sizes. Furthermore, the high and relatively rapid ZnONP dissolution in aqueous media makes detection by SP-ICP-MS challenging, due to a significant overlap of the dissolved Zn (i) and NP signals. So, in the tests conditions, the method was not able to detect particles less than $67 \pm 2 \text{ nm}$, which corresponds to a mass detection limit (LODm) equivalent to 874 ag. Those results are in accordance with literature, and it is suitable for validation process (29). Additionally, this result was experimentally confirmed through the analysis of 10 independent replicates of the blank sample and calculated by the simplified method, showing the results are statistically equal (7, 10).

The concentration of the number of particles mL^{-1} was calculated using the number of particles (events), considering the total aspirated solution volume during the time analysis. LODp was 1.08×10^5 particles mL^{-1} , and was determined using a sample flow of 0.2 mL min^{-1} , TE (8,3%), and aquisition time (100s) (27). These results are in accordance with the literature (7, 10).

The limit of quantification (LOQ) for Zn(i) was obtained experimentally, defined as the first point of the calibration curve ($1 \mu\text{g L}^{-1}$). The values are suitable for this study and present adequate sensitivity for the applied technique.

Accuracy and precision

To evaluate the method accuracy and precision, two types of samples were selected: reference material Nist Water 1643F and a recovery study in sunscreen sample, considering ZnO is frequently employed in physical blocker sunscreens. Five independent solutions of each sample were prepared and analyzed in single particle mode. The average number of particles determined for each standard and the concentration of dissolved ions were compared with the expected values. The results are shown in Table 2. The Zn(i) concentration was chosen to be close to the middle of the range of calibration curve ($10 \mu\text{g L}^{-1}$), and the ZnNP concentration (1.08×10^5 particles mL^{-1}).

Table 2

Accuracy and precision evaluation for dissolved zinc and zinc oxide nanoparticles (ZnONPs), determined in single particle detection mode (n = 5)

Sample	Added Zn(i) $\mu\text{g L}^{-1}$	Measured Zn (i) $\mu\text{g L}^{-1}$	Added ZnONP partcles mL^{-1}	Measured ZnONP partcles mL^{-1}	Most Frequent Size (nm)	%REC	% RSD
Nist 1643F	--	8.7 ± 1.5	--	$< 1.08 \times 10^5$	< 67	Zn(i) 120%	16
Nist 1643F	10	17.3 ± 1.2	1.08×10^5	1.2×10^6	89	Zn(i) - 93% ZnONP 107%	Zn(i) - 7 ZnONP- 30
Sunscreen	--	12.1 ± 2.8	-	$< 1.08 \times 10^5$	< 67	--	Zn(i) - 28 ZnONP - -
Sunscreen	10	18.3 ± 1.6	1.08×10^5	$8.6 \times 10^5 \pm 3.9 \times 10^4$	78	Zn(i)- 83% ZnONP 88%	Zn(i) - 9 ZnONP - 45
Note: Zn(i), zinc ions; % REC, per cent recovered measured for Zn(i) in $\mu\text{g L}^{-1}$ and ZnO partcles mL^{-1} ; % RSD, per cent relative standard deviation; - not added and/or measured.							

The accuracy study makes possible to conclude that ZnONP was present in the evaluated samples. However, the concentration of dissolved Zn ($> 10 \mu\text{g L}^{-1}$) was higher than the number of ZnONP particles, which is equivalent to a concentration of $0.43 \mu\text{g L}^{-1}$, so the Zn(i) signal overlaps the nanoparticles signal, directly interfering in the analyses. Under these conditions, only very large particles or agglomerates can be distinguished from dissolved Zn. This result is consistent with other studies in the literature (30, 32), and this phenomenon is observed especially at lower particle concentrations, in the range of 1.0×10^5 (33). As for Zn(i) recovery, the results are in accordance with the settled by INMETRO in the established working range.

In the evaluation of the size of the nanoparticles, we can observe for the reference material Nist -Water 1643F the size is within the range declared in the certificate, which informs the suspension has nanoparticles smaller than 100 nm, with the predominant size of 75 nm. The reference material Nist Water 1643F had a higher NP numbers and sizes than the added, which can be attributed to a higher background interference in this material, since this sample has a known concentration of Zn(i) (14). For the sunscreen sample, after addition, the size became larger, possibly due to agglomeration, caused by

the matrix complexity and the presence of Zn(i) which increased the base signal. Furthermore, there is significant variation between the results that can be observed by the RSD (14).

This methodology was applied in sunscreen and water samples in this work nonetheless other studies show that this technique has already been applied to samples as cosmetics, food products, and textiles containing ZnONPs. This diversification demonstrates the method's applicability and robustness in detecting and quantifying NPs across different matrices. Furthermore, other articles comparing SP-ICP-MS results with those obtained from established techniques such as TEM and DLS. This comparative analysis confirms the accuracy and precision of the SP-ICP-MS technique, showcasing its reliability for nanoparticle analysis in complex matrices (23, 34, 35).

Determination of size distribution of nanoparticle

The solution containing nanoparticles presented larger size frequency, 89 nm zinc oxide particles and a concentration of $9.92 \times 10^4 \text{ mL}^{-1}$ particles. Table 3 presents the distribution of particles by size range and Fig. 2 presents the histograms of the size distribution of the sample.

Table 3
Distribution by size range and most frequent size in sample the reference material – Nist Water 1643F

Distribution by size (nm)	Most Frequent Size (nm)	% NPs
0–20	0	0
21–40	0	0
41–60	0	0
61–80	78	1
81–100	89	68
100–120	106	17
> 120	122	13

Method uncertainty

To estimate the uncertainty associated with Zn(i) concentration, the only factor that will have no influence is transport efficiency (TE). The result for expanded measurement uncertainty for Zn(i) concentration determination in the single particle mode was 4%. The uncertainty associated with the calibration curve was 20%. Regarding the determining of the size of the NPs, the expanded uncertainty was 33% (Fig. 5), and the uncertainty that most contributed was the sample preparation (58%) and TE (25%). The uncertainty determination associated with transport efficiency, was estimated at 1% relative to its standard deviation, considered the contribution related to analysis time (min). This estimation was performed because it was not possible to determine experimental parameters, and the software does

not provide this information, standard concentration, and repeatability. The uncertainty that most contributed to the estimated combined uncertainty for TE was the uncertainty associated with the concentration of the standard, which shows the demand to work with certified materials with low uncertainty, since they are responsible for the TE that will influence the entire analysis in single particulate mode.

Conclusions

The SP-ICP-MS technique demonstrated good selectivity for determining Zn(i), ZnONP in single particle mode and the results obtained in the method validation meet all requirements, to the established INMETRO guidelines for analytical methods. Moreover the uncertainty analysis provided insights into factors influencing the SP-ICP-MS technique's accuracy, particularly highlighting the role of transport efficiency. However, the challenge of distinguishing between dissolved ions and NP signals, especially for smaller NPs, was noted. This limitation underscores the necessity for ongoing methodological enhancements, such as employing ion exchange resins or reaction cells to minimize this interference.

In addition, by expanding which this technique can be used in different samples and employing comparative analyses with other established techniques, we offer a comprehensive approach that enhances the understanding and application of SP-ICP-MS in nanoparticle analysis.

This study contributes significantly to strengthening the knowledge about the application of nanotechnology, providing data for future studies and practical applications in nanotechnology, thereby supporting quality control and regulatory standards for products containing nanomaterials.

Declarations

Ethical Approval - not applicable

Funding - not applicable

Availability of data and materials- not applicable

Acknowledgments

The authors are grateful to the following Brazilian agencies: Coordenação de Aperfeiçoamento de Pessoal de Nível superior - Brasil (CAPES) - Finance Code 001, Fundação Carlos Chagas Filho de Amparo a Pesquisa do Estado do Rio de Janeiro-FAPERJ (Grant: Rede NanoSaúde-E-26/2010.1/2019; E-26/2010.255/2020), INOVA/Fiocruz and Project LabVisa for financial support, Anvisa and UCSF/CTRE Briger fellowship.

The statements and opinions expressed in the article are those of the authors and are based on current scientific evidence. They do not represent any institutional guideline and/or opinion of Anvisa, FIOCRUZ, the Ministry of Health and/or the Brazilian Government.

Author Contributions

Lisia M. G. dos Santos: Conceptualization, Data curation, , Investigation, Project administration, Resources, Validation, Visualization, Writing original draft, Writing-review e Editing; *Cristiane Barata-Silva*: Conceptualization, Data curation, Investigation, Project administration, Resources, Validation, Visualization, Writing original draft, Writing-review e Editing; *Santos A. V. Neto*: Investigation, Resources, Validation, Visualization, Writing-review e Editing; *Fabio S. Bazilio*: Visualization, Writing-review e Editing; *Renata A Pereira*: Investigation, Resources, Validation; *André Luiz O da Silva*: Writing-review e Editing; *Josino C. Moreira*: Conceptualization, Formal analysis funding acquisition, Project administration, Writing-review e Editing; *Silvana C. Jacob*: Conceptualization, Formal analysis funding acquisition, Project administration, Writing-review e Editing.

References

1. Bayda S, Adeel M, Tuccinardi T, Cordani M, Rizzolio F. The History of Nanoscience and Nanotechnology: From Chemical–Physical Applications to Nanomedicine. *Molecules*. 27 de dezembro de 2019;25(1):112.
2. Ahire SA, Bachhav AA, Pawar TB, Jagdale BS, Patil AV, Koli PB. The Augmentation of nanotechnology era: A concise review on fundamental concepts of nanotechnology and applications in material science and technology. *Results Chem*. 1º de janeiro de 2022;4:100633.
3. Smijs TG, Pavel S. Titanium dioxide and zinc oxide nanoparticles in sunscreens: focus on their safety and effectiveness. *Nanotechnol Sci Appl*. 13 de outubro de 2011;4:95–112.
4. Wiechers JW, Musee N. Engineered Inorganic Nanoparticles and Cosmetics: Facts, Issues, Knowledge Gaps and Challenges. *J Biomed Nanotechnol*. 1º de outubro de 2010;6(5):408–31.
5. Jiang J, Pi J, Cai J. The Advancing of Zinc Oxide Nanoparticles for Biomedical Applications. *Bioinorg Chem Appl*. 5 de julho de 2018;2018:e1062562.
6. Grasso A, Ferrante M, Moreda-Piñeiro A, Arena G, Magarini R, Oliveri Conti G, et al. Dietary exposure of zinc oxide nanoparticles (ZnO-NPs) from canned seafood by single particle ICP-MS: Balancing of risks and benefits for human health. *Ecotoxicol Environ Saf*. 1º de fevereiro de 2022;231:113217.
7. Laborda F, Jiménez-Lamana J, Bolea E, Castillo JR. Selective identification, characterization and determination of dissolved silver(I) and silver nanoparticles based on single particle detection by inductively coupled plasma mass spectrometry. *J Anal At Spectrom*. 1º de julho de 2011;26(7):1362–71.
8. Hayder M, Wojcieszek J, Asztemborska M, Zhou Y, Ruzik L. Analysis of cerium oxide and copper oxide nanoparticles bioaccessibility from radish using SP-ICP-MS. *J Sci Food Agric*. 2020;100(13):4950–8.
9. Strenge I, Engelhard C. Single particle inductively coupled plasma mass spectrometry: investigating nonlinear response observed in pulse counting mode and extending the linear dynamic range by

- compensating for dead time related count losses on a microsecond timescale. *J Anal At Spectrom.* 2 de janeiro de 2020;35(1):84–99.
10. Laborda F, Jiménez-Lamana J, Bolea E, Castillo JR. Critical considerations for the determination of nanoparticle number concentrations, size and number size distributions by single particle ICP-MS. *J Anal At Spectrom.* 11 de julho de 2013;28(8):1220–32.
 11. Donovan AR, Shi H, Stephan C. Rapid Analysis of Silver, Gold, and Titanium Dioxide Nanoparticles in Drinking Water by Single Particle ICP-MS.
 12. Bolea-Fernandez E, Leite D, Rua-Ibarz A, Liu T, Woods G, Aramendia M, et al. On the effect of using collision/reaction cell (CRC) technology in single-particle ICP-mass spectrometry (SP-ICP-MS). *Anal Chim Acta.* 24 de outubro de 2019;1077:95–106.
 13. Laborda F, Bolea E, Jiménez-Lamana J. Single particle inductively coupled plasma mass spectrometry for the analysis of inorganic engineered nanoparticles in environmental samples. *Trends Environ Anal Chem.* 1º de janeiro de 2016;9:15–23.
 14. de la Calle I, Menta M, Klein M, Séby F. Screening of TiO₂ and Au nanoparticles in cosmetics and determination of elemental impurities by multiple techniques (DLS, SP-ICP-MS, ICP-MS and ICP-OES). *Talanta.* 15 de agosto de 2017;171:291–306.
 15. Mozhayeva D, Engelhard C. A critical review of single particle inductively coupled plasma mass spectrometry – A step towards an ideal method for nanomaterial characterization. *J Anal At Spectrom.* 2 de setembro de 2020;35(9):1740–83.
 16. Meermann B, Nischwitz V. ICP-MS for the analysis at the nanoscale – a tutorial review. *J Anal At Spectrom.* 30 de agosto de 2018;33(9):1432–68.
 17. Laborda F, Abad-Álvaro I, Jiménez MS, Bolea E. Catching particles by atomic spectrometry: Benefits and limitations of single particle - inductively coupled plasma mass spectrometry. *Spectrochim Acta Part B At Spectrosc.* 1º de janeiro de 2023;199:106570.
 18. ABNT. ISO. 2017 [citado 10 de fevereiro de 2024]. Associação brasileira de normas técnicas. NBR ISO/IEC 17025/2017: Requisitos gerais para a competência de laboratórios de ensaio e calibração. Disponível em: <https://www.iso.org/standard/66912.html>
 19. INMETRO. Instituto Nacional de Metrologia, Qualidade e Tecnologia. Orientação sobre validação de métodos analíticos. Documento de caráter orientativo. DOQ-CGCRE-008. Revisão 09 - JUN/2020. 2020.
 20. Method Validation [Internet]. [citado 14 de abril de 2024]. Disponível em: <https://www.eurachem.org/index.php/publications/guides/mv>
 21. 14:00–17:00. ISO. [citado 14 de abril de 2024]. ISO/TS 19590:2017. Disponível em: <https://www.iso.org/standard/65419.html>
 22. Donovan AR, Adams CD, Ma Y, Stephan C, Eichholz T, Shi H. Detection of zinc oxide and cerium dioxide nanoparticles during drinking water treatment by rapid single particle ICP-MS methods. *Anal Bioanal Chem.* 1º de julho de 2016;408(19):5137–45.

23. Fréchette-Viens L, Hadioui M, Wilkinson KJ. Quantification of ZnO nanoparticles and other Zn containing colloids in natural waters using a high sensitivity single particle ICP-MS. *Talanta*. 1º de agosto de 2019;200:156–62.
24. Geiss O, Bianchi I, Bucher G, Verleysen E, Brassinne F, Mast J, et al. Determination of the Transport Efficiency in spICP-MS Analysis Using Conventional Sample Introduction Systems: An Interlaboratory Comparison Study. *Nanomaterials*. janeiro de 2022;12(4):725.
25. Santos LMG dos, Barata-Silva C, Vicentini Neto SA, Fonseca MA, Magalhães CD, Moreira JC, et al. Analytical method validation for the identification and quantification of dissolved gold and gold nanoparticles in cosmetics products by single particle inductively coupled plasma mass spectrometry. *Quím Nova*. 11 de agosto de 2021;44:760–5.
26. Laborda F, Gimenez-Ingalaturre AC, Bolea E, Castillo JR. About detectability and limits of detection in single particle inductively coupled plasma mass spectrometry. *Spectrochim Acta Part B At Spectrosc*. 1º de julho de 2020;169:105883.
27. dos Santos LMG, Barata-Silva C, Neto SAV, Magalhães CD, Moreira JC, Jacob SC. Analysis and risk assessment of arsenic in rice from different regions of Brazil. *J Food Compos Anal*. 1º de junho de 2021;99:103853.
28. Witzler M, Küllmer F, Hirtz A, Günther K. Validation of Gold and Silver Nanoparticle Analysis in Fruit Juices by Single-Particle ICP-MS without Sample Pretreatment. *J Agric Food Chem*. 25 de maio de 2016;64(20):4165–70.
29. Bazilio FS, dos Santos LMG, Silva CB, Neto SAV, Senna CA, Archanjo BS, et al. Migration of silver nanoparticles from plastic materials, with antimicrobial action, destined for food contact. *J Food Sci Technol*. 1º de fevereiro de 2023;60(2):654–65.
30. Bazilio FS, Bomfim MVJ, Almeida RJ, Abrantes SMP. Uso de Planilha eletrônica na verificação da adequação de curva analítica ao modelo linear. *Analytica São Paulo*. 2012;50(59):60–7.
31. Bazilio FS, Silva CB, Santos LMG dos, Neto SAV, Jacob S do C, Abrantes S de MP. DETECÇÃO E QUANTIFICAÇÃO DE NANOPARTÍCULAS DE PRATA POR spICP-MS. *Quím Nova*. 3 de setembro de 2021;44:868–73.
32. De la Calle I, Menta M, Séby F. Current trends and challenges in sample preparation for metallic nanoparticles analysis in daily products and environmental samples: A review. *Spectrochim Acta Part B At Spectrosc*. 1º de novembro de 2016;125:66–96.
33. Ma R, Levard C, Judy JD, Unrine JM, Durenkamp M, Martin B, et al. Fate of Zinc Oxide and Silver Nanoparticles in a Pilot Wastewater Treatment Plant and in Processed Biosolids. *Environ Sci Technol*. 7 de janeiro de 2014;48(1):104–12.
34. Pusuwan P, Siripinyanond A. Observing zinc oxide nanoparticles suspension stability in various media by using single particle inductively coupled plasma mass spectrometry (SP-ICP-MS). *Microchem J*. 1º de janeiro de 2024;196:109705.

35. Suwanroek W, Sumranjit J, Wutikhun T, Siripinyanond A. Use of single particle inductively coupled plasma mass spectrometry for the study of zinc oxide nanoparticles released from fabric face masks. *J Anal At Spectrom.* 6 de abril de 2022;37(4):759–67.

Figures

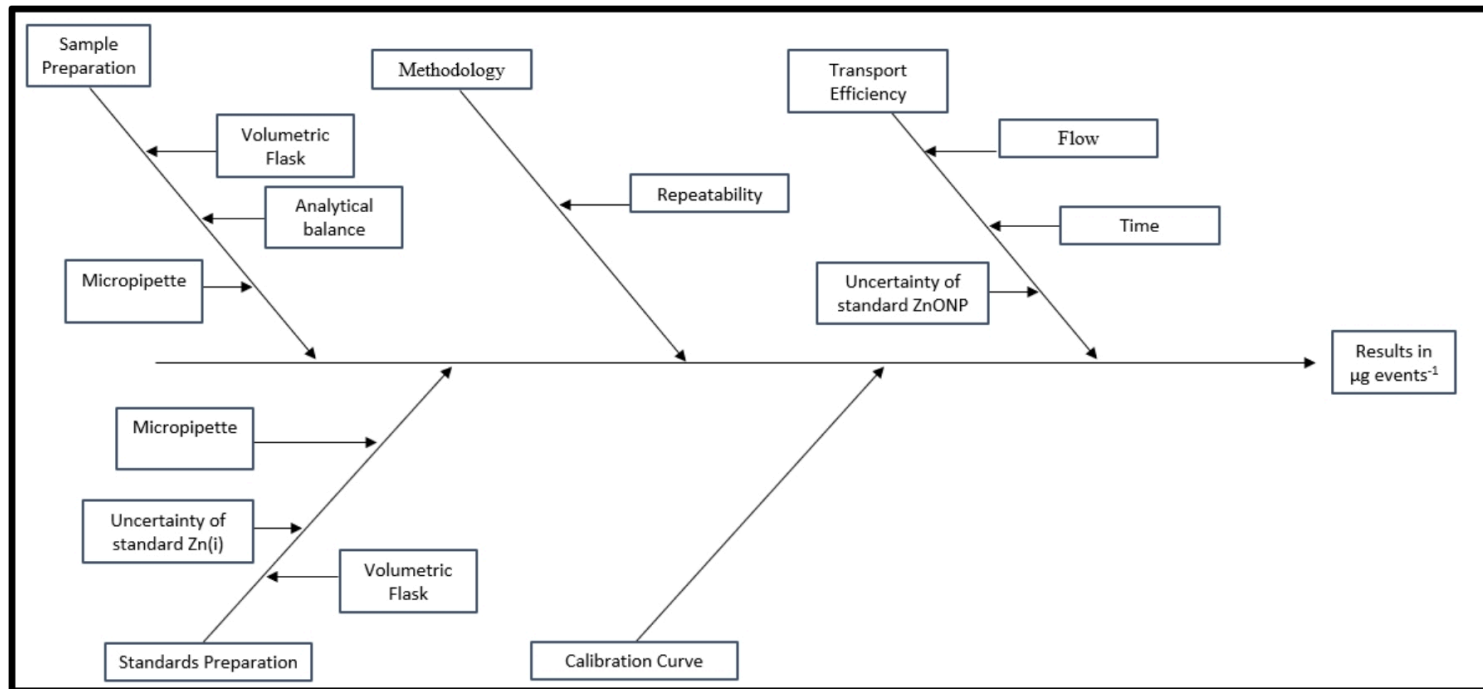


Figure 1

Cause and effect diagram with the parametrs that affect the method uncertainty for identification of size of nanoparticle

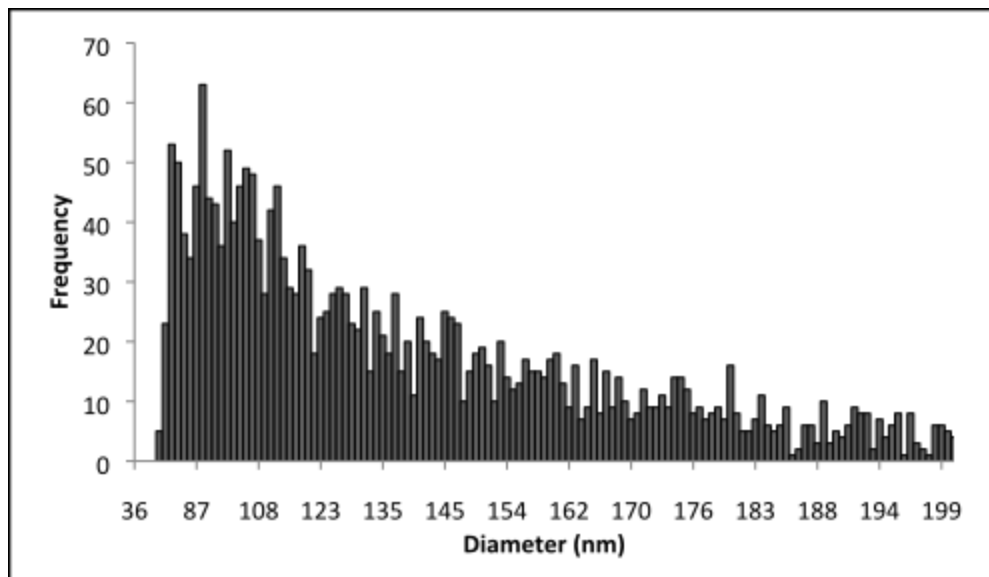


Figure 2

Histogram of the particle size distribution of the reference material Nist Water 643F added with ZnONP (size < 100nm)

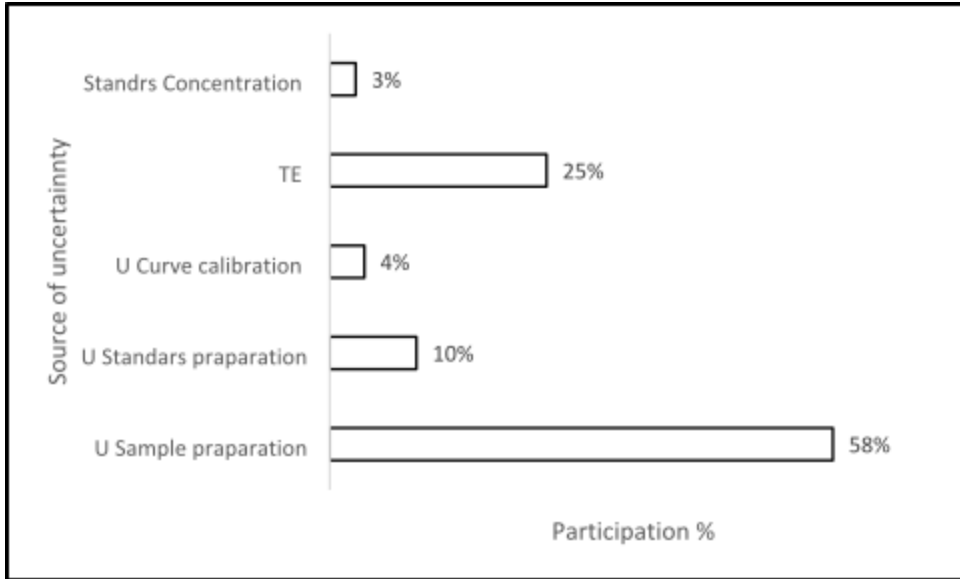


Figure 3

Contribution of uncertainty sources, estimated by the classical method for sunscreen sample added with ZnONP (size < 100nm), to the estimated combined uncertainty for part. mL⁻¹.